College of Pharmacy[1], Chengdu Medical College, Chengdu; College of Pharmacy[2], Chongqing University, Chongqing, China

Cyanidin-3-*O*-glucoside chloride acts synergistically with luteolin to inhibit the growth of colon and breast carcinoma cells

Huanli Yin[1,#], Langtao Wang[1,2,#], Min Wu[1,*], Yuan Liu[1], Ningxi Li[1], Tianyu Chen[1]

Received September 2, 2018, accepted October 8, 2018

**Corresponding author: Min Wu, College of Pharmacy, Chengdu Medical College, Chengdu, 610500, Sichuan, China*
wuminzhaofeng@126.com
[#]These authors contributed equally to this work.

Pharmazie 74: 54–61 (2019) *doi: 10.1691/ph.2019.8746*

In this study, we investigated whether the combination of cyanidin-3-*O*-glucoside chloride and luteolin could inhibit the growth of HCT-8 colon and MCF-7 breast carcinoma cells, and whether the effect of the combination was greater than the effect of either drug on its own. Growth inhibition was assessed using the CCK-8 assay, level of apoptosis and cell cycle distribution were determined using flow cytometry, and the mechanism of apoptosis induction was explored using a colorimetric assay of caspases-3 and -9. Experiments indicated that combination treatment inhibited proliferation and increased apoptosis in both cell lines to a greater extent than either drug on its own. These results suggest that luteolin and cyanidin-3-*O*-glucoside chloride synergistically inhibitthe growth of colon cancer and breast cancer cells. This work justifies further effort to develop this potential combination therapy.

1. Introduction

Cancer is a leading cause of mortality worldwide, so efforts to treat cancer and reduce associated mortality are a priority (Dutta and Mahato 2017). Chemotherapy is an essential strategy against cancer, but many drugs cause severe side effects (Waller et al. 2015), in part because most chemotherapeutic drugs target all cells that are rapidly dividing, not only cancer cells. This leads to toxic effects particularly in normal cells that actively proliferate, such as in bone marrow, gastrointestinal tract and hair follicles. Efforts are needed to identify and develop more effective and less toxic chemotherapeutic agents, as well as identify appropriate combinations of agents that can counteract the complex pathology of cancer and metastasis more effectively than single agents (Lockhart et al. 2015). Combination therapy also sometimes allows the use of lower doses of single agents, which can reduce toxicity (Kumari et al. 2016; Yardley 2013; Zhan et al. 2014), and it can help to overcome drug resistance (Leslie et al. 2001).

Natural products with anti-cancer effects, such as vincristine, camptothecine, doxorubicin, dactinomicine, mitomycin and bleomycin , are of considerable interest because they are often more effective and less toxic than synthetic drugs. Flavonoids, polyphenolic compounds found ubiquitously in plants, show therapeutic effects against many disease states, including cancer, cardiovascular disease, and neurodegenerative disorders (Di et al. 1999; Fiorani and Accorsi 2005; Verschooten et al. 2012). They are often included in food additives and health food supplements and are considered active ingredients in many herbal medicines (Coleta et al. 2008). The flavonoid luteolin (Lu), which is 3',4', 5,7-tetrahydroxyflavone (Fig. 1A), is an active compound from *Rosmarinus officinalis* (Lamiaceae) (El Omri et al. 2012). It shows a range of pharmacological properties (Hemanta Majumder et al. 2002), including the ability to inhibit angiogenesis and proliferation in tumors, arrest tumor cells in G1 and G2/M and induce apoptosis. Lu can also exert anti-oxidant effects and mitigate the toxicity of anti-tumor drugs (Zhu et al. 2017) .

Another natural product with strong anti-tumor activity is the anthocyanin cyanidin-3-*O*-glucoside (C3G, Fig. 1B). This is the main anthocyanin in the edible parts of several plants, and it shows a range of beneficial effects (Ding et al. 2006; Sasaki et al. 2007). It inhibits proliferation, inflammation, angiogenesis and invasion in esophageal, colon, skin, and lung cancer, and it induces apoptosis (Wang and Stoner 2008).

Our own computational studies (data not shown) suggest that Lu and C3G bind to different targets to exert their effects. In other reports, Lu inhibits DNA topoisomerase I or vascular endothelial cells in tumors (Chowdhury et al. 2002; Topcu et al. 2008), and it prevents adhesion of tumor cells to vascular endothelial cells, hindering metastasis (Bagli et al. 2004). C3G, in contrast, inhibits glyoxalase I, the rate-limiting enzyme in the process through which cancer cells inactivate the pro-apoptotic agent methylglyoxal (Takasawa et al. 2010). These contrasting mechanisms suggest that the combination of C3G and Lu may be more effective than either agent alone at inhibiting the proliferation and metastasis of cancer cells, which is indeed predicted by our *in silico* studies (data not shown).

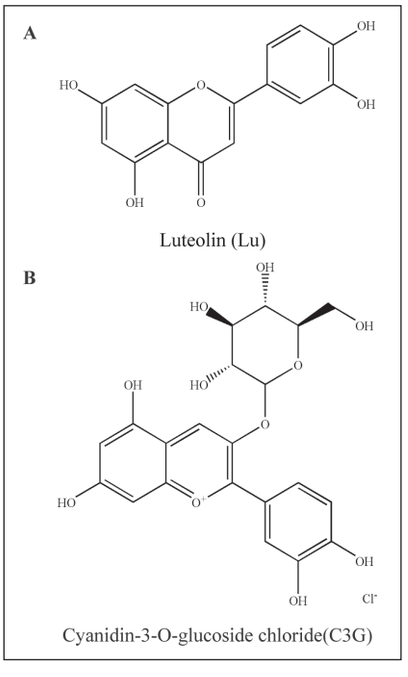

Fig. 1: Chemical structures of (A) luteolin and (B)cyanidin-3-*O*-glucoside.

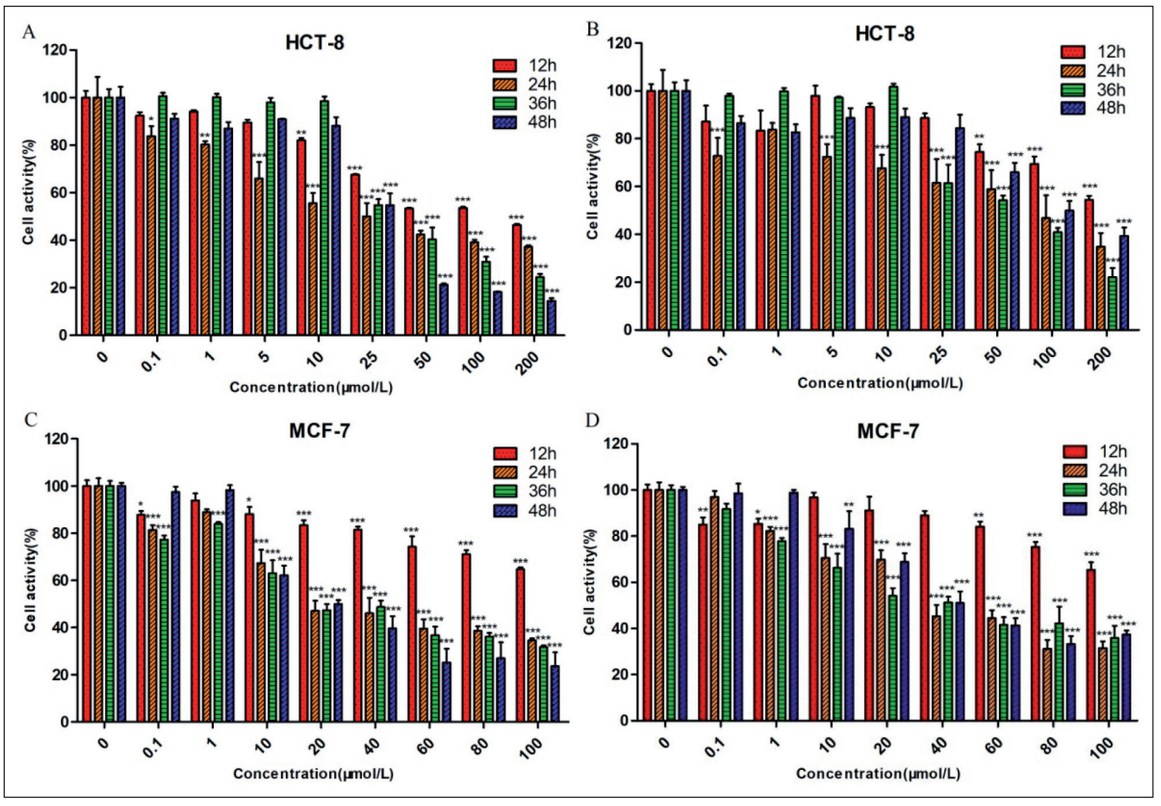

Fig. 2: C3G and Lu on their own reduc eviability of colon and breast carcinoma cells. (A, C) Effect of different doses of luteolin on viability of colon carcinoma and breast cancer cells after 12, 24, 36 or 48h. (B, D) Effect of different doses of cyanidin-3-*O*-glucoside on colon carcinoma and breast cancer cell viability after 12, 24, 36 or 48h. Cell viability was assessed using the CCK-8 assay and expressed as a percentage of control cultures.*p<0.05, **p<0.01 and ***p<0.001 vs. control cultures (two-way ANOVA).

To examine the efficacy of Lu-C3G therapy experimentally, we applied the agents alone or in combination to cultures of colon and breast cancer cells. Our results suggest that even at low doses, combining the two agents leads to synergistic anti-tumor effects.

2. Investigations and results

2.1. Effects of Lu and C3G on proliferation of HCT-8 and MCF-7 cells

Viability of HCT-8 colon carcinoma cells and MCF-7 breast cancer cells exposed to Lu, C3G or both was assessed using the CCK-8 assay. Viability was lower in all treatment groups than in the negative control group, and the reduction was concentration- and time-dependent (Fig. 2). The drugs exerted maximal effects with both cell lines at 24 h. IC_{50} values, defined as the concentrations that inhibited cell growth by 50% relative to the negative control, were determined at 24 h from dose-response curves. Against HCT-8 cells, IC_{50} was 20 μM for Lu (Fig. 2A) and 70 μM for C3G (Fig. 2C). The corresponding values against MCF-7 cells were 16 μM for Lu (Fig. 2B) and 40 μM for C3G (Fig. 2D).

In both cell lines, the combination of Lu and C3G reduced cell viability more than either agent on its own (Fig. 3A). Analysis of the combination index showed a potent synergy of cell killing in both cell lines for two of the six agent combinations, which fell on the lower left of the isobologram (Fig. 3B-C). Co-treatment with Lu and C3G synergistically inhibited cell growth in ratios of 2:7 and 3:8 in HCT-8 cells and in ratios of 2:5 and 1:2 in MCF-7 cells. When the two drugs were applied to the cell lines in fixed ratios of 2:7 HCT-8 cells and 2:5 in MCF-7 cells respectively, synergistic reduction in cell viability was observed for two of the six combinations in HCT-8 cells and four of the six combinations in MCF-7 cells (Fig. 4).

2.2. Effects of Lu and C3G on migration of HCT-8 cells

Next we used a wound healing assay to investigate whether the combination of drugs can suppress migration of HCT-8 cells better than either agent alone. The agents, alone or in combination, reduced migration, although the combination did not reduce migration synergistically (Fig. 5).

2.3. Effects of Lu and C3G on cell cycle progression in HCT-8 and MCF-7 cells

We used flow cytometry to compare the cell cycle distribution of HCT-8 and MCF-7 cells treated for 24 h with Lu and/or C3G. We used doses equal to the corresponding IC_{50} values or higher. While either agent on its own showed negligible effects on the cell cycle distribution of both cell lines, the combination increased the sub-G1 population of HCT-8 cells (Fig. 6A). This result suggests that combining the two agents can induce apoptosis. In addition, we found that Lu can arrest MCF-7 cells in G2 phase (Fig. 6B).

2.4. Effects of Lu and C3G on morphology of HCT-8 and MCF-7 cells

To investigate whether cellular apoptosis is involved in the cytotoxicity of the combination of Lu and C3G, we observed the two cell lines after drug treatment and nuclear staining with Hoechst 33258 (Fig. 7). Cells treated with the agents alone or together showed chromatin condensation as well as nuclear fragmentation and shrinkage, indicating apoptosis. Numbers of dead cells and extent of apoptotic chromatin condensation were greater in cells treated with both agents than in cells treated with either agent alone.

2.5. Synergistic induction of apoptosis of HCT-8 and MCF-7 cells by Lu and C3G

To confirm that the anti-tumor effects of Lu and C3G were associated with induction of apoptosis, HCT-8 cells were treated with the agents alone or in combination, subjected to Annexin V/propidium iodide (PI) double staining and sorted based on apoptotic stage using flow cytometry. The agents alone or combined

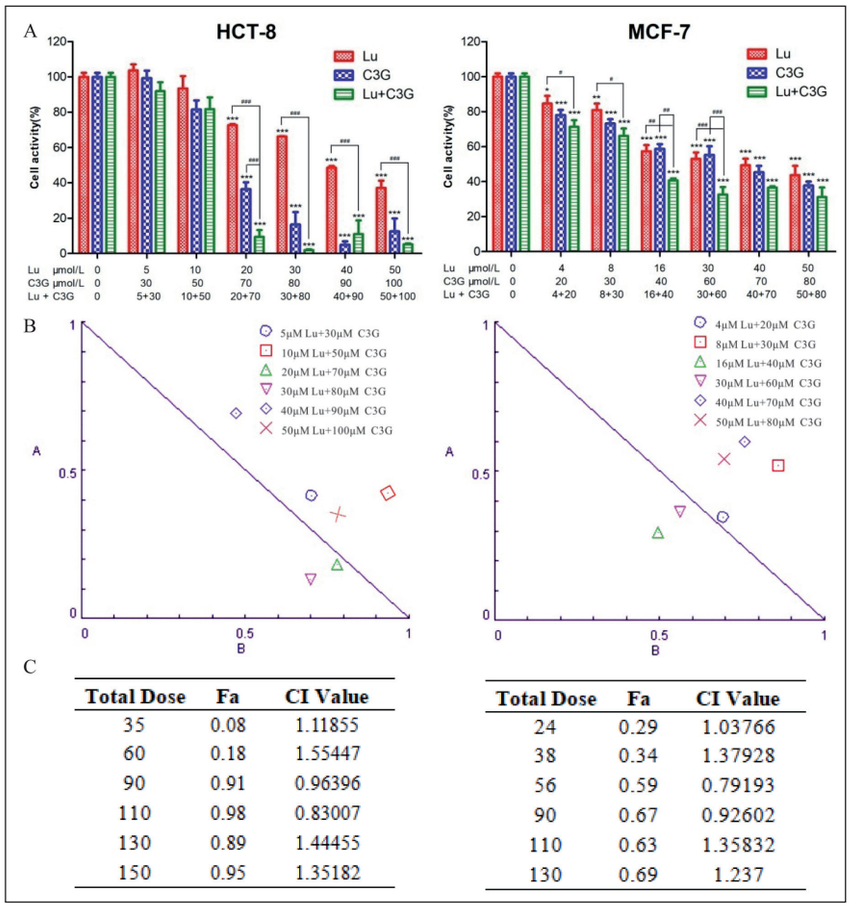

Total Dose	Fa	CI Value
35	0.08	1.11855
60	0.18	1.55447
90	0.91	0.96396
110	0.98	0.83007
130	0.89	1.44455
150	0.95	1.35182

Total Dose	Fa	CI Value
24	0.29	1.03766
38	0.34	1.37928
56	0.59	0.79193
90	0.67	0.92602
110	0.63	1.35832
130	0.69	1.237

Fig. 3: C3G and Lu synergistically reduced the viability of colon and breast carcinoma cells. (A) Effect of the combination of different doses of C3G and Lu on the viability of colon and breast carcinoma cells after 24 h. *p<0.05, **p<0.01, ***p<0.001 vs. the corresponding control. #p<0.05, ##p<0.01, ###p<0.001 referring to the difference between Lu or C3G alone and LC (two-way ANOVA). (B) Isobologram representation of cell viability after treatment with the combination of drugs. CI, combination index. (C) CI describing drug interaction at different concentrations.

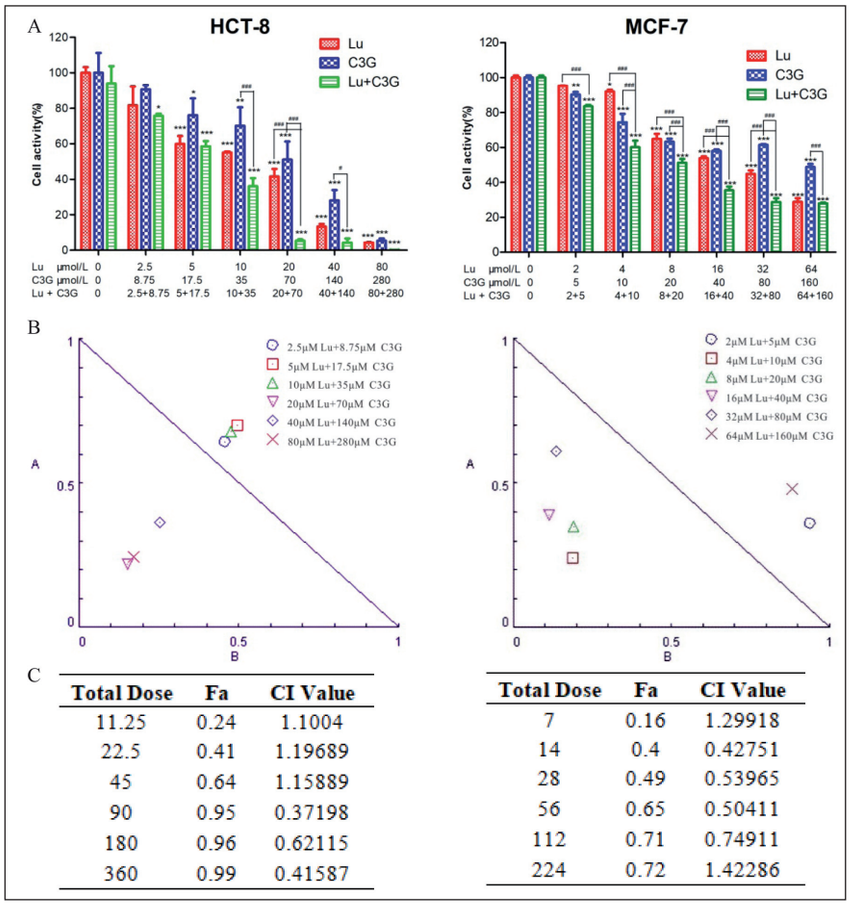

Total Dose	Fa	CI Value
11.25	0.24	1.1004
22.5	0.41	1.19689
45	0.64	1.15889
90	0.95	0.37198
180	0.96	0.62115
360	0.99	0.41587

Total Dose	Fa	CI Value
7	0.16	1.29918
14	0.4	0.42751
28	0.49	0.53965
56	0.65	0.50411
112	0.71	0.74911
224	0.72	1.42286

Fig. 4: C3G and Lu synergistically reduced viability of colon and breast carcinoma cells. (A) Effect of the combination of different doses of C3G and Lu on the viability of colon and breast carcinoma cells after 24 h. *p<0.05, **p<0.01, ***p<0.001 vs. the corresponding control. #p<0.05, ##p<0.01, ###p<0.001 referring to the difference between Lu or C3G alone and LC (two-way ANOVA). (B) Isobologram representation of cell viability after treatment with the combination of drugs. (C) CI describing drug interaction at different concentrations.

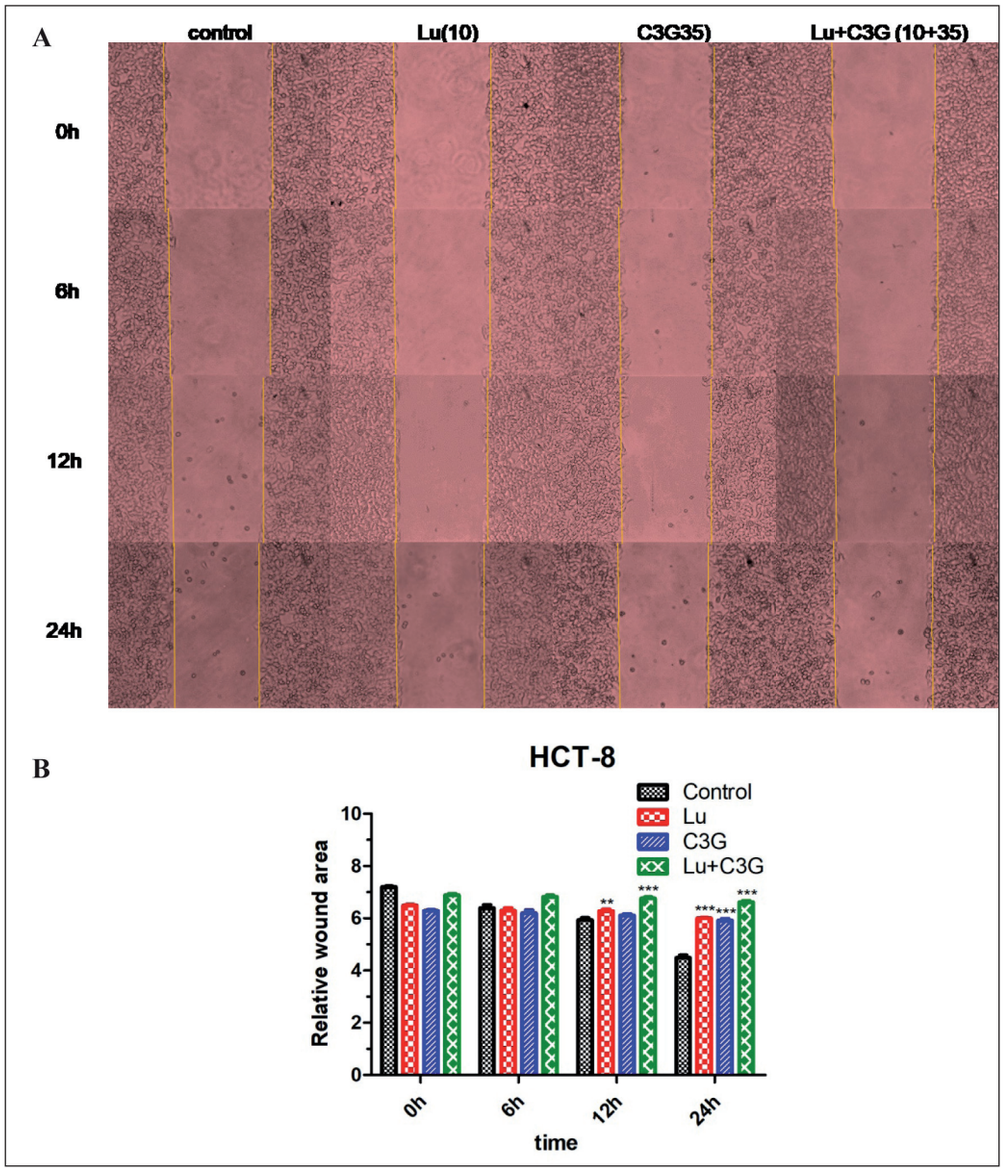

Fig. 5: Effects of C3G and Lu on wound healing by HCT-8 cells. (A) Phase-contrast microscopy was used to observe the linear scratch through the cell monolayer (10×) at the indicated times (0, 6, 12, 24 h) after scratching. Cultures were treated as follows: control; Lu at 10 µmol/L; C3G at 35 µmol/L; C3G and Lu at 10 and 35µmol/L, respectively. (B)Wound areas were calculated using Image-Pro Plus 6.0 software. **p<0.05, ***p<0.001 referring to the difference between treated and control cells (two-way ANOVA).

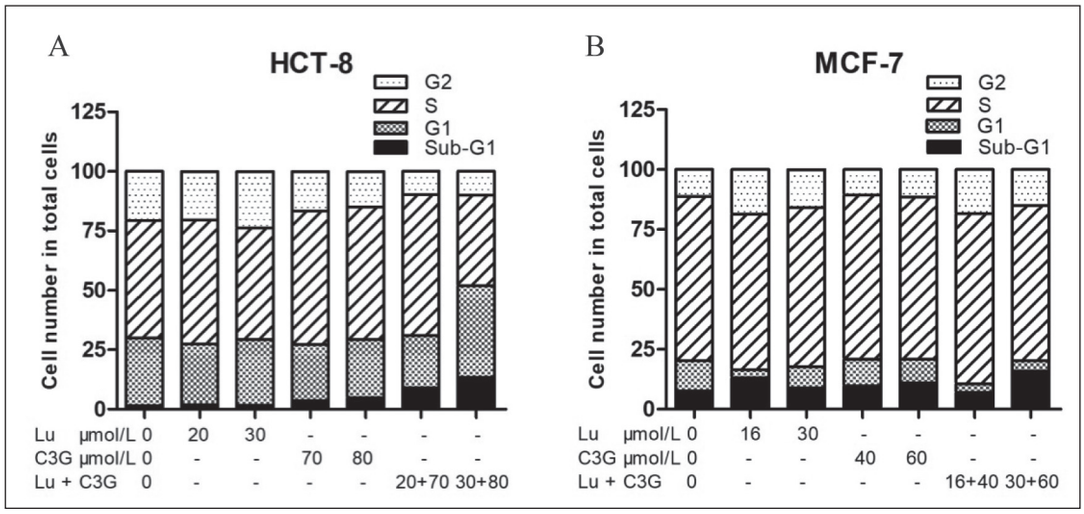

Fig. 6: Cell cycle progression in HCT-8 and MCF-7 cells treated for 24 h with different doses of C3G, Lu or both. Cells were stained with propidium iodide (PI) and analyzed by flow cytometry to determine distributions in the cell cycle, which are indicated in columns in the diagram.

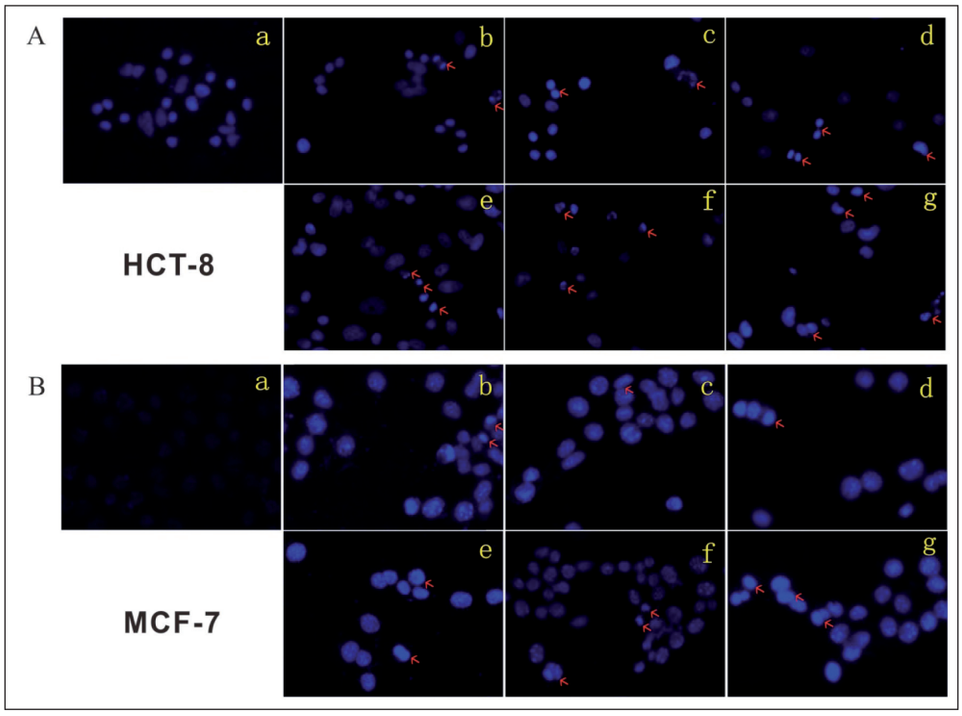

Fig. 7: Cellular apoptosis observed with Hoechst 33258 staining (magnification, 20×). (A)HCT-8 cells were treated for 24 h with Lu, C3G or both. Small arrows indicate chromatin condensation, nuclear fragmentation and apoptotic bodies. Cultures were treated as follows: (a) control group, (b) Lu (20 μmol/L), (c) C3G (70 μmol/L), (d) Lu (20 μmol/L)+C3G (70 μmol/L), (e) Lu (40 μmol/L), (f) C3G (140 μmol/L), (g) Lu (40 μmol/L)+C3G (140 μmol/L). (B) MCF-7 cells were treated for 24 h with Lu, C3G or both. Small arrows indicate chromatin condensation, nuclear fragmentation and apoptotic bodies. Cultures were treated as follows: (a) control, (b) Lu (16 μmol/L), (c) C3G (40 μmol/L), (d) Lu (16 μmol/L)+C3G (40 μmol/L), (e) Lu (32 μmol/L), (f) C3G (80 μmol/L), (g) Lu (32 μmol/L)+C3G (80 μmol/L). Experiments were conducted in triplicate and carried out at least three times.

significantly increased the proportion of apoptotic cells, and the proportion was significantly higher after combination treatment than after monotherapy (Fig. 8). Analysis of the combination index showed a potent synergy of apoptosis induction at three of the four combinations, which fell on the lower left of the isobologram (Fig. 8B-C). As in the case of HCT-8 cells, treating MCF-7 cells with Lu and C3G significantly increased the apoptotic population (Fig. 9). These results are consistent with the idea that induction of apoptosis helps mediate the synergistic toxicity of Lu and C3G against colon and breast cancer cells.

2.6. Effects of Lu and C3G on activation of caspases-3 and -9 in HCT-8 and MCF-7 cells

To gain insights into how the combination of Lu and C3G induces apoptosis, we exposed the cell lines to lower doses that showed synergy in the *in vitro* experiments described above. In HCT-8 cells, caspase-3 activity was significantly higher in cells treated with 20 μM Lu + 70 μM CG3 or 30 + 80 μM than in negative control cells ($P < 0.001$; Fig. 10). In MCF-7 cells, our results suggest that the combination may promote apoptosis by increasing expression of caspases-3 and -9 (Fig. 10).

3. Discussion

The present study evaluated the synergistic effects of Lu and C3G on HCT-8 and MCF-7 cells. To the best of our knowledge, this is the first *in vitro* study about the ability of C3G to inhibit proliferation and metastasis of HCT-8 colon carcinoma cells. Our results argue for the potential of Lu-C3G combination therapy to treat colon and breast cancers. Further studies are needed to explore the safety and efficacy of this combination.

Our results are consistent with the known ability of Lu to inhibit tumor proliferation (Kang et al. 2003; Zhang et al. 2005), migration and invasion, cell cycle progression, angiogenesis (Ambasta et al. 2015), and inflammation. They also support the ability of Lu to induce apoptosis (Cai et al. 2011; Kang et al. 2017; Lim et al. 2007). Our results are consistent with the known ability of C3G to inhibit proliferation of various types of tumor cells (Shih et al. 2007; Wang and Stoner 2008; Xu et al. 2010). We extend this knowledge by showing that the combination of Lu and C3G was much more effective than either agent alone at inhibiting the growth of HCT-8 or MCF-7 cells. At several doses, the two agents acted synergistically based on analysis of the combination index (Figs. 3-4) and of morphological changes in treated cells. In fact, this appears to be the first report of synergy between C3G and Lu in inducing apoptosis in HCT-8 cells (Fig. 8).

Lu was previously found to inhibit angiogenesis and proliferation in HT-29 human colon cancer cells (Ambasta et al. 2015). In these cells, Lu arrests cells in G1 and G2/M by inhibiting the activity of CDK2, CDK4, and CDC2 (Lim et al. 2007). In HT-29 cells, Lu exerts apoptotic effects by promoting antioxidant activity and activating MAPK signaling . In HCT-15 human colon cancer cells, Lu inhibits Wnt/β-catenin signaling, induces apoptosis, and arrests cells in G2/M (Pandurangan et al. 2013). In A549 cells, Lu can inhibit cell growth and induce G2 arrest and apoptosis by activating JNK and inhibiting translocation of NF-κB (p65)(Cai et al. 2011). C3G can induce apoptosis in HEK-293 cells by inhibiting activation of the NF-kB signaling pathway (Liu et al. 2017). In HS578T cells, C3G can inhibit growth and proliferation by arresting cells at the G2/M phase as well as inducing apoptosis (Chen et al. 2005). In MDA-MB-453 breast cancer cells, C3G induces apoptosis via Bcl-2 and Bax pathways (Cho et al. 2017). In highly metastatic A549 human lung carcinoma cells, it inhibits migration and invasion by down-regulating matrix metalloproteinase-2 and urokinase plasminogen activator, upregulating tissue inhibitor of matrix metalloproteinase-2 and plasminogen activator inhibitor, and inhibiting the activation of c-Jun and NF-kB (Chen et al. 2006). Future studies should examine whether one or more of these pathways also mediate the anti-tumor effects observed here with combination therapy of C3G and Lu.

C3G and Lu possess intrinsic luminescence, which may allow them to function as fluorescent small-molecule probes that can be detected sensitively with assay systems that can measure mercapto-containing molecules. Such probes may be useful for measuring physiology and pathology of proteins and other species in their native environments.

In summary, the present study showed that the combination of Lu and C3G inhibited proliferation and increased apoptosis in HCT-8 and MCF-7 cells to a greater extent than either agent on its own. The synergistic anti-tumor effects of these agents layed a solid foundation for further development of this combination regimen into an effective therapy against colorectal and breast cancers.

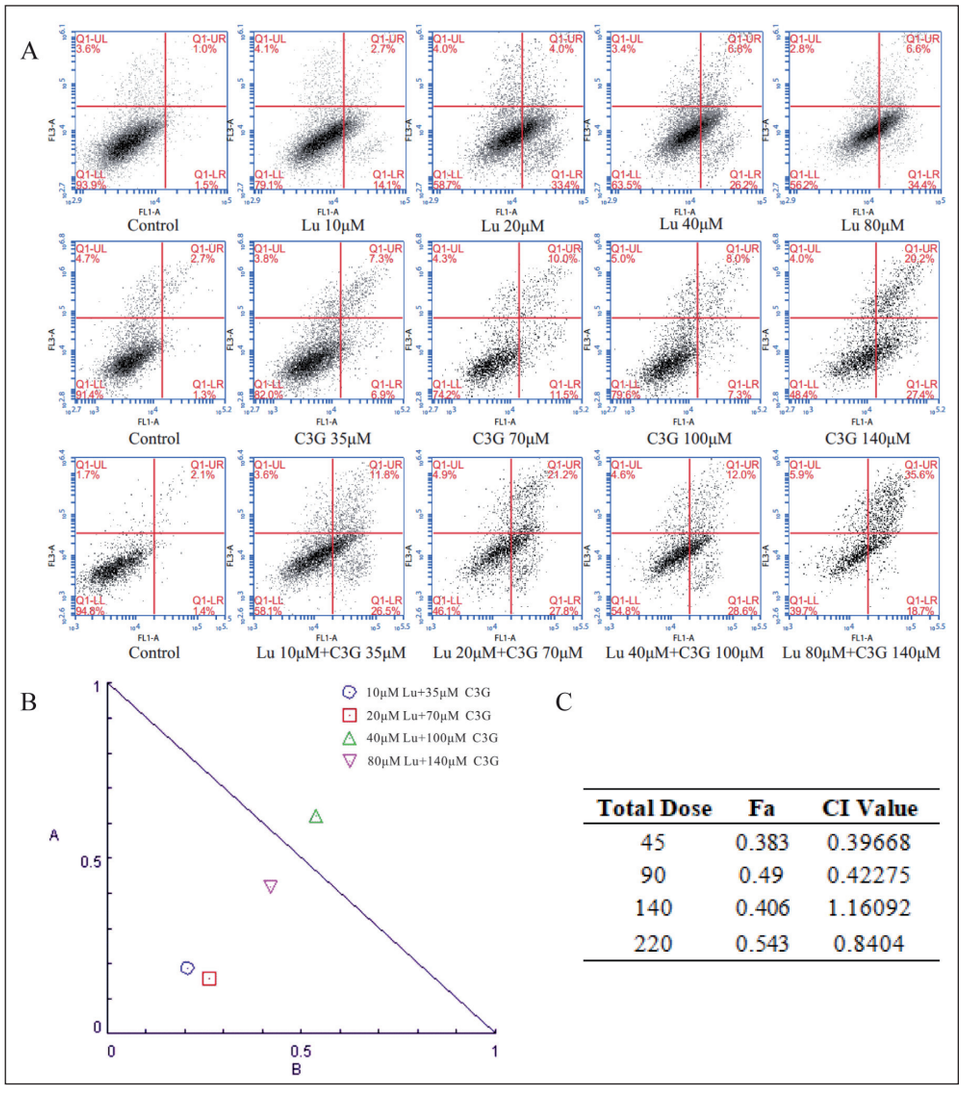

Total Dose	Fa	CI Value
45	0.383	0.39668
90	0.49	0.42275
140	0.406	1.16092
220	0.543	0.8404

Fig. 8: Apoptosis of HCT-8 cells mediated by C3G and Lu, alone or in combination. (A) Apoptosis was measured by flow cytometry after PI/Annexin V-FITC staining. Q1-upper left, PI+ (cells undergoing necrosis); Q1-upper right, Annexin V-FITC+ PI+ (cells in late apoptosis and secondary necrosis); Q1-lower right, Annexin V-FITC+PI- (cells in early apoptosis); Q1-lower left, Annexin V-FITC- PI- (living cells). Total apoptotic rate was calculated as upper right+ lower right. (B) Isobologram of apoptosis induction by the combination of both drugs. (C) Combination index (CI) describing drug interaction at different concentrations.

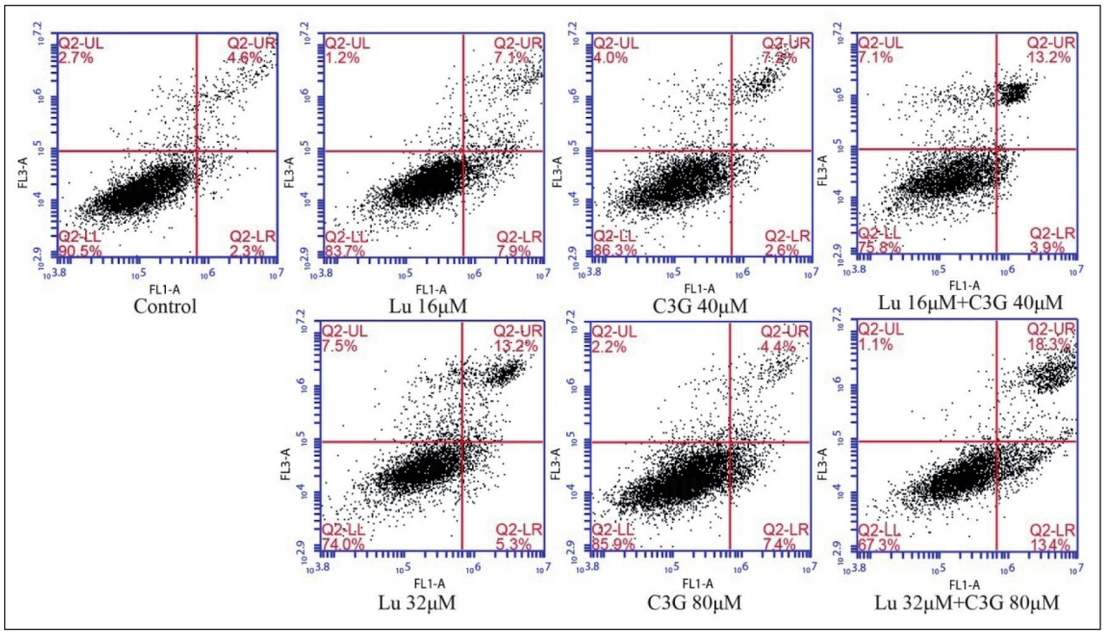

Fig. 9: Apoptosis of MCF-7 cells induced by C3G and Lu, alone or in combination. Apoptosis was measured by flow cytometry after PI/Annexin V-FITC staining. Q2-upper left, PI+ (cells undergoing necrosis); Q2-upper right, Annexin V-FITC+ PI+ (cells in late apoptosis and secondary necrosis); Q2-lower right, Annexin V-FITC+ PI- (cells in early apoptosis); Q2-lower left, Annexin V-FITC- PI- (living cells). Total apoptotic rate was calculated as upper right+ lower right.

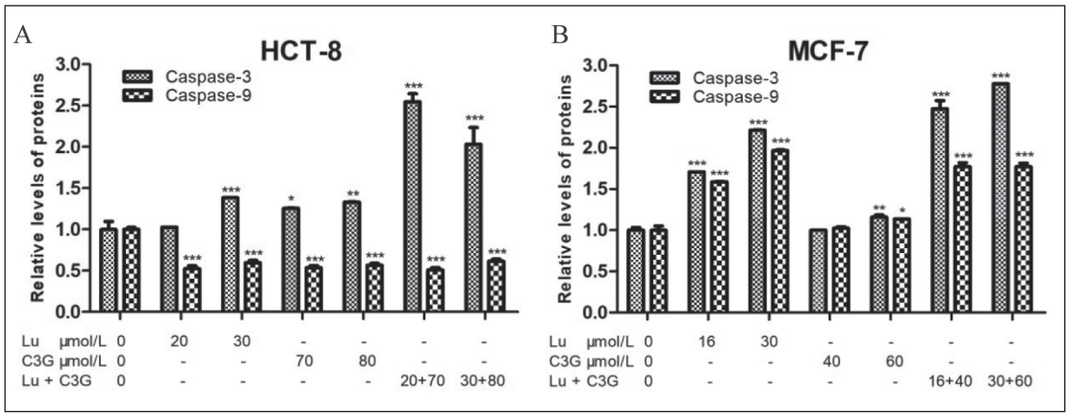

Fig. 10: Fluorometric assay of caspase activity in HCT-8 and MCF-7 cells treated for 24 h with C3G, Lu or both (0-100 μM). Cell lysates were prepared and aliquots (100 μg) analyzed for caspase activity using fluorometric substrates for caspases-3 and -9. Fluorescence intensity is shown relative to that in the untreated control.

4. Experimental

4.1. Lu and C3G

Lu was purchased from Xi'an Ainuo Pharmaceutical Technology (Xi'an, China) and dissolved in DMSO. C3G was obtained from Sichuan Weikeqi Biological Technology (Chengdu, China), dissolved in DMSO, and stored in the dark. These agents were used in experiments at concentrations ranging from 0.1 to 200 mM. DMSO (99.5%) was purchased from BioFroxx GmbH (Einhausen , Germany).

4.2. Cell lines and culture

HCT-8 human colon carcinoma cells were purchased from Procell Life Science & Technology (Wuhan, China). MCF-7 human breast carcinoma cells were kindly provided by Dr. Changyang Gong at the Department of pharmacy, Sichuan University (Chengdu, China). HCT-8 cells were incubated at 37 °C in a humidified atmosphere with 5 % CO_2 and cultured in RPMI-1640 medium (HyClone, Logan City, UT, USA) containing 10 % fetal bovine serum (Gibco, Grand Island, NY, USA) supplemented with 1 % non-essential amino acids and 100 IU/ml penicillin G sodium and 100 μg/ml streptomycin sulfate (Solarbio Technology, Beijing, China). MCF-7 cells were cultured in DMEM supplemented as described for RPMI-1640.

4.3. CCK-8 assay

Cell viability was determined using the Cell Counting Kit-8 (CCK-8) assay (KeyGen Biotech, Nanjing, China). HCT-8 or MCF-7 cells were seeded into 96-well plates (5×10^3 per well) in a final volume of 100 μl and incubated for 12 h at 37 °C in a humidified atmosphere containing 5 % CO_2, then the medium was replaced with fresh medium containing various concentrations of Lu or C3G alone, and plates were incubated another 12, 24, 36, or 48 h. To examine synergistic effects between the two agents, cells were allowed to attach as above, then incubated with the agents alone or in combination in fresh medium, and plates were incubated another 24 h. The number of viable cells was determined at the end of the incubation period using the CCK-8 kit according to the manufacturer's instructions. Absorbance at 450 nm was read using a microplate reader (VERSA max; Molecular Devices, Sunnyvale, CA, USA). Survival was quantified according to the equation

$$\text{Survival index} = (OD_{experimental} - OD_{blank}) / (OD_{control} - OD_{blank}) \times 100\%,$$

where OD refers to optical density. Measurements were adjusted for absorbance of negative control wells without cells. All data reported here are from at least three independent experiments.

4.4. Wound healing assay

Effects of Lu and CG3 on cancer cell migration were measured in a wound healing assay, in which a scratch is made in a confluent cell monolayer, and then the extent to which cells establish new cell-cell contacts and close the gap is measured (Liang et al. 2007). Cells were seeded into 6-well plates (5×10^4 per well) in a final volume of 1000 μl and allowed to attach for 12 h. After cells had reached confluence, the medium was aspirated and a pipette tip approximately 1 mm wide was used to scratch the monolayer. Then fresh RPMI-1640 containing various concentrations of Lu, C3G or both was added, and plates were incubated for the indicated times at 37 °C in a humidified atmosphere containing 5 % CO_2. A phase-contrast microscope (IX71S1F-3, Olympus Optical, Tokyo, Japan) was used to observe the linear wound in the monolayer at 0, 6, 12 and 24 h.

4.5. Flow cytometry for cell cycle distribution

Flow cytometry was used to detect the distribution of cells across the cell cycle (Carmo et al. 2011). Cells were seeded into 6-well culture plates ($5x10^5$ per well), cultured in the presence or absence of the indicated agents, harvested in 0.25 % trypsin, collected and fixed at 4 °C overnight with cold 70 % ethanol. Then, the cells were centrifuged at 1000 *g* for 5 min and incubated for 60 min at 37 °C in 0.5 ml propidium iodide (KeyGen Biotech, Nanjing, China) containing 0.1 mg/ml RNaseA (KeyGen Biotech, Nanjing, China). Data were acquired and analyzed using a NovoCyte 3130 flow cytometry system (ACEA Biosciences, San Diego, CA, USA) and NovoExpress 1.2.5 software.

4.6. Apoptosis staining using Hoechst 33258

Clean cover slips were soaked in 70 % ethanol for at least 5 min, washed three times with sterile phosphate-buffered saline (PBS), and washed again with the fresh culture medium. Cover slips were then placed in culture dishes measuring 60 × 20 mm, cells were seeded into the dishes, and the dishes were incubated overnight until they had reached 50-80% confluence. Cells were treated for 24 h at 37 °C with Lu, C3G or both. The medium was aspirated, then 0.5 ml of fixative was added, and cells were fixed for at least 10 min. Cells were washed twice, stained for 15 min at room temperature with Hoechst 33258 (Beyotime Institute of Biotechnology, Shanghai, China), and again washed twice. A drop of anti-fluorescence quenching mounting solution was placed on a slide and covered with the cell-coated cover slip to allow the cells to contact the mounting fluid and avoid air bubbles. Cell morphology was observed and images were captured from random visual fields using phase-contrast fluorescence microscopy (Model IX71S1F-3, Olympus Optical, Tokyo, Japan). Fluorescence was measured at an excitation wavelength of 350 nm and an emission wavelength of 460 nm.

4.7. Flow cytometry to assess apoptosis levels

Cells were seeded into 12-well plates (10^5 per well) and cultured in the presence or absence of the indicated agents, harvested using 0.25 % trypsin and collected, centrifuged at 1000 rpm/min for 5 min, washed twice in PBS and resuspended in 500 μl Binding Buffer (KeyGen Biotech, Nanjing, China). Apoptosis was evaluated at 15 min following treatment using an apoptosis detection kit (KeyGen Biotech, Nanjing, China) based on staining with fluorescein isothiocyanate-conjugated Annexin V and propidium iodide at 25 °C in the dark. Fluorescence was measured at an excitation wavelength of 488 nm and an emission wavelength of 530 nm on a flow cytometer (BD Biosciences, San Jose, CA, USA). The entire process was completed within one hour.

4.8. Colorimetric assay to measure pro-apoptotic activation of caspases-3 and -9 (Kumar 2004)

After treatment, cells were harvested and lysed with Lysis Buffer supplemented with dithiothreitol (DTT) (KeyGen Biotech). Protein concentration was determined using the Bradford protein quantitation assay. Aliquots of approximately 100 μg protein were suspended in 2x Reaction Buffer with DTT, then incubated at 37 °C for 4 h with caspase-3 or -9 substrate (KeyGen Biotech). Absorbance was measured at 405 nm using a microplate reader as described in section 4.3. Relative protein expression was calculated according to the formula:

$$\text{Relative protein expression} = (OD_{experimental} - OD_{blank}) / (OD_{control} - OD_{blank}).$$

4.9. Combined drug analysis

Interaction between Lu and C3G was assessed using the combination index-isobologram equation, based on a two-drug pharmacologic interaction model . A combination index of 1 indicates an additive effect; <1, synergism; and >1, antagonism. Dose-response curves and the combination index were calculated using Compusyn© 1.0 (ComboSyn, Paramus, NJ, USA).

4.10. Statistical analysis

Data were expressed as mean value±SEM. Differences between groups were assessed for significance using two-way ANOVA in GraphPad Prism 5.0 (San Diego, CA, USA). Differences associated with $p < 0.05$ were considered significant, unless stated otherwise.

Acknowledgments: This work was supported by the National Natural Science Foundation of China (81372424), the Key Fund Project of the Sichuan Provincial Department of Education (17ZA0110) and the Sichuan Provincial College Students Innovation and Entrepreneurship Training Program (201613705054).

Conflicts of interest: None declared.

References

Ambasta RK, Jha SK, Kumar D, Sharma R, Jha NK, Kumar P (2015) Comparative study of anti-angiogenic activities of luteolin, lectin and lupeol biomolecules. J Transl Med 13: 307:

Bagli E, Stefaniotou M, Morbidelli L, Ziche M, Psillas K, Murphy C, Fotsis T (2004) Luteolin inhibits vascular endothelial growth factor-induced angiogenesis; inhibition of endothelial cell survival and proliferation by targeting phosphatidylinositol 3'-kinase activity. Cancer Res 64: 7936-7946.

Cai X, Ye T, Liu C, Lu W, Lu M, Zhang J, Wang M, Cao P (2011) Luteolin induced G2 phase cell cycle arrest and apoptosis on non-small cell lung cancer cells. Toxicol in Vitro 25: 1385-1391.

Carmo A, Carvalheiro H, Crespo I, Nunes I, Lopes MC (2011) Effect of temozolomide on the U-118 glioma cell line. Oncol Lett 2: 1165-1170.

Chen P, Chu S, Chiou H, Chiang C, Yang S, Hsieh Y (2005) Cyanidin 3-glucoside and peonidin 3-glucoside inhibit tumor cell growth and induce apoptosis in vitro and suppress tumor growth in vivo. Nutr Cancer 53: 232-243.

Chen PN, Chu SC, Chiou HL, Kuo WH, Chiang CL, Hsieh YS (2006) Mulberry anthocyanins, cyanidin 3-rutinoside and cyanidin 3-glucoside, exhibited an inhibitory effect on the migration and invasion of a human lung cancer cell line. Cancer Lett 235: 248-259.

Cho E, Chung EY, Jang HY, Hong OY, Chae HS, Jeong YJ, Kim SY, Kim BS, Yoo DJ, Kim JS, Park KH (2017) Anti-cancer effect of cyanidin-3-glucoside from mulberry via caspase-3 cleavage and DNA fragmentation in vitro and in vivo. Anticancer Agents Med Chem 17: 1519-1525.

Chou TC, Martin N (2007) The mass-action law-based new computer software, CompuSyn, for automated simulation of synergism and antagonism in drug combination studies. Cancer Res 67; Abstract 637:

Chou TC (2010) Drug combination studies and their synergy quantification using the Chou-Talalay method. Cancer Res 70: 440-446.

Chowdhury ASS, Mandal S, Goswami A, Mukhopadhyay S, Majumder HK (2002) Luteolin, an emerging anti-cancer flavonold, poisons eukaryotic DNA topoisomerase I. Biochem J 366: 653-661.

Coleta M, Campos MG, Cotrim MD, Lima TCMD, Cunha APD (2008) Assessment of luteolin (3′,4′,5,7-tetrahydroxyflavone) neuropharmacological activity. Behav Brain Res 189: 75-82.

Di CG, Mascolo N, Izzo AA, Capasso F (1999) Flavonoids: old and new aspects of a class of natural therapeutic drugs. Life Sci 65: 337-353.

Ding M, Feng R, Wang SY, Bowman L, Lu Y, Qian Y, Castranova V, Jiang B, Shi X (2006) Cyanidin-3-glucoside, a natural product derived from blackberry, exhibits chemopreventive and chemotherapeutic activity. J Biol Chem 281: 17359-17368.

Dutta R, Mahato RI (2017) Recent advances in hepatocellular carcinoma therapy. Pharmacol Ther 173: 106-117.

EL Omri A, Han J, Kawada K, Ben Abdrabbah M, Isoda H (2012) Luteolin enhances cholinergic activities in PC12 cells through ERK1/2 and PI3K/Akt pathways. Brain Res 1437: 16-25.

Fiorani M, Accorsi A (2005) Dietary flavonoids as intracellular substrates for an erythrocyte trans-plasma membrane oxidoreductase activity. Brit J Nutr 94: 338-345.

Hemanta Majumder K, Sharma S, Mandal S, Goswami A, Mukhopadhyay S, Majumder HK (2002) Luteolin, an emerging anti-cancer flavonoid, poisons eukaryotic DNA topoisomerase I. Biochem J 366: 653-661.

Kang KA, Piao MJ, Ryu YS, Hyun YJ, Park JE, Shilnikova K, Zhen AX, Kang HK, Koh YS, Jeong YJ, Hyun JW (2017) Luteolin induces apoptotic cell death via antioxidant activity in human colon cancer cells. Int J Oncol 51: 1169-1178.

Kang SY, Seeram NP, Nair MG, Bourquin LD (2003) Tart cherry anthocyanins inhibit tumor development in Apc(Min) mice and reduce proliferation of human colon cancer cells. Cancer Lett 194: 13-19.

Kumar S (2004) Measurement of caspase activity in cells undergoing apoptosis. Methods Mol Biol 282: 19-30.

Kumari S, Badana A, Gayatridevi V, Nagaseshu P, Varalakshmi M, Malla RR (2016) Coralyne targets proteases involved in cancer progression: An in silico study. In: Lakshmi P., Zhou W., Satheesh P. (eds) Computational Intelligence Techniques in Health Care. SpringerBriefs in Applied Sciences and Technology. Springer, Singapore, pp. 19-30.

Leslie EM, Mao Q, Oleschuk CJ, Deeley RG, Cole SP (2001) Modulation of multidrug resistance protein 1 (MRP1/ABCC1) transport and atpase activities by interaction with dietary flavonoids. Mol Pharmacol 59: 1171-1180.

Liang C, Park AY, Guan J (2007) In vitro scratch assay: a convenient and inexpensive method for analysis of cell migration in vitro. Nat Protoc 2: 329-333.

Lim DY, Jeong Y, Tyner AL, Park JHY (2007) Induction of cell cycle arrest and apoptosis in HT-29 human colon cancer cells by the dietary compound luteolin. Am J Physiol Gastr Liver Physiol 292: G66-G75.

Liu D, Wang Y, Ma S, Sun H, Shi W, Feng X (2017) Individual and combined use of ginsenoside F2 and cyanidin-3-O-glucoside attenuates H2O2-induced apoptosis in HEK-293 cells via the NF-κB pathway. RSC Adv 7: 41713 – 41722.

Lockhart JN, Stevens DM, Beezer DB, Kravitz A, Harth E (2015) Dual drug delivery of tamoxifen and quercetin: Regulated metabolism for anticancer treatment with nanosponges. J Control Release 220: 751-757.

Sasaki R, Nishimura N, Hoshino H, Isa Y, Kadowaki M, Ichi T, Tanaka A, Nishiumi S, Fukuda I, Ashida H, Horio F, Tsuda T (2007) Cyanidin 3-glucoside ameliorates hyperglycemia and insulin sensitivity due to downregulation of retinol binding protein 4 expression in diabetic mice. Biochem Pharmacol 74: 1619-1627.

Shih P, Yeh C, Yen G (2007) Anthocyanins induce the activation of phase II enzymes through the antioxidant response element pathway against oxidative stress-induced apoptosis. J Agr Food Chem 55: 9427-9435.

Singh CK, George J, Ahmad N (2013) Resveratrol-based combinatorial strategies for cancer management. Ann NY Acad Sci 1290: 113–121.

Takasawa R, Saeki K, Tao A, Yoshimori A, Uchiro H, Fujiwara M, Tanuma S (2010) Delphinidin, a dietary anthocyanidin in berry fruits, inhibits human glyoxalase I. Bioorgan Med Chem 18: 7029-7033.

Topcu Z, Ozturk B, Kucukoglu O, Kilinc E (2008) Flavonoids in Helichrysum pamphylicum inhibit mammalian type I DNA topoisomerase. Zschr Naturforsch C 63: 69-74.

Verschooten L, Barrette K, Van Kelst S, Rubio RN, Proby C, De Vos R, Agostinis P, Garmyn M (2012) Autophagy inhibitor chloroquine enhanced the cell death inducing effect of the flavonoid luteolin in metastatic squamous cell carcinoma cells. PLoS One 7: e48264.

Waller LP, Deshpande V, Pyrsopoulos N (2015) Hepatocellular carcinoma: A comprehensive review. World J Hepatol 7: 2648-2663.

Wang L, Stoner GD (2008) Anthocyanins and their role in cancer prevention. Cancer Lett 269: 281-290.

Xu M, Bower KA, Wang S, Frank JA, Chen G, Ding M, Wang S, Shi X, Ke Z, Luo J (2010) Cyanidin-3-Glucoside inhibits ethanol-induced invasion of breast cancer cells overexpressing ErbB2. Mol Cancer 9: 1-14.

Yardley DA (2013) Drug resistance and the role of combination chemotherapy in improving patient outcomes. Int J Breast Cancer 2013: 137414.

Zhan Y, Chen Y, Liu R, Zhang H, Zhang Y (2014) Potentiation of paclitaxel activity by curcumin in human breast cancer cell by modulating apoptosis and inhibiting EGFR signaling. Arch Pharm Res 37: 1086-1095.

Zhang Y, Vareed SK, Nair MG (2005) Human tumor cell growth inhibition by nontoxic anthocyanidins, the pigments in fruits and vegetables. Life Sci 76: 1465-72.

Zhu B, Yu L, Yue Q (2017) Co-delivery of vincristine and quercetin by nanocarriers for lymphoma combination chemotherapy. Biomed Pharmacother 91: 287-294.